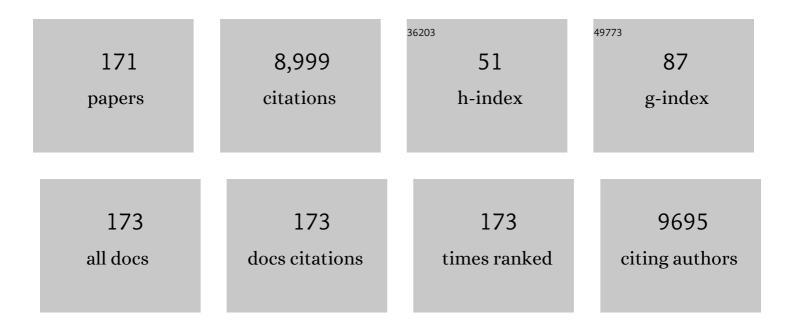
List of Publications by Year in descending order

Source: https://exaly.com/author-pdf/9170854/publications.pdf Version: 2024-02-01



#	Article	IF	CITATIONS
1	Core–shell nanoparticles: synthesis and applications in catalysis and electrocatalysis. Chemical Society Reviews, 2015, 44, 7540-7590.	18.7	906
2	Challenges and Recent Advances in High Capacity Liâ€Rich Cathode Materials for High Energy Density Lithiumâ€lon Batteries. Advanced Materials, 2021, 33, e2005937.	11.1	253
3	Toward noble-metal-free visible-light-driven photocatalytic hydrogen evolution: Monodisperse sub–15 nm Ni2P nanoparticles anchored on porous g-C3N4 nanosheets to engineer 0D-2D heterojunction interfaces. Applied Catalysis B: Environmental, 2018, 221, 47-55.	10.8	251
4	Achieving Fast and Durable Lithium Storage through Amorphous FeP Nanoparticles Encapsulated in Ultrathin 3D P-Doped Porous Carbon Nanosheets. ACS Nano, 2020, 14, 9545-9561.	7.3	250
5	Sub-5 nm Ultra-Fine FeP Nanodots as Efficient Co-Catalysts Modified Porous g-C ₃ N ₄ for Precious-Metal-Free Photocatalytic Hydrogen Evolution under Visible Light. ACS Applied Materials & Interfaces, 2019, 11, 5651-5660.	4.0	208
6	Designing Polymerâ€inâ€Salt Electrolyte and Fully Infiltrated 3D Electrode for Integrated Solidâ€State Lithium Batteries. Angewandte Chemie - International Edition, 2021, 60, 12931-12940.	7.2	202
7	Double-shell Li-rich layered oxide hollow microspheres with sandwich-like carbon@spinel@layered@spinel@carbon shells as high-rate lithium ion battery cathode. Nano Energy, 2019, 59, 184-196.	8.2	194
8	High performance columnar-like Fe2O3@carbon composite anode via yolk@shell structural design. Journal of Energy Chemistry, 2020, 41, 126-134.	7.1	191
9	Preparation and magnetic properties of nickel nanoparticles via the thermal decomposition of nickel organometallic precursor in alkylamines. Nanotechnology, 2007, 18, 505703.	1.3	187
10	Ni ₁₂ P ₅ nanoparticles embedded into porous g-C ₃ N ₄ nanosheets as a noble-metal-free hetero-structure photocatalyst for efficient H ₂ production under visible light. Journal of Materials Chemistry A, 2017, 5, 16171-16178.	5.2	183
11	Lithium Deficiencies Engineering in Li-Rich Layered Oxide Li _{1.098} Mn _{0.533} Ni _{0.113} Co _{0.138} O ₂ for High-Stability Cathode. Journal of the American Chemical Society, 2019, 141, 10876-10882.	6.6	171
12	Recent Advances and Strategies toward Polysulfides Shuttle Inhibition for Highâ€Performance Li–S Batteries. Advanced Science, 2022, 9, e2106004.	5.6	161
13	Construction of network-like and flower-like 2H-MoSe2 nanostructures coupled with porous g-C3N4 for noble-metal-free photocatalytic H2 evolution under visible light. Applied Catalysis B: Environmental, 2018, 233, 26-34.	10.8	147
14	Hierarchical ZnIn ₂ S ₄ /MoSe ₂ Nanoarchitectures for Efficient Nobleâ€Metalâ€Free Photocatalytic Hydrogen Evolution under Visible Light. ChemSusChem, 2017, 10, 4624-4631.	3.6	140
15	Yolk-shell ZnO-C microspheres with enhanced electrochemical performance as anode material for lithium ion batteries. Electrochimica Acta, 2014, 125, 659-665.	2.6	137
16	Surface Partial-Charge-Tuned Enhancement of Catalytic Activity of Platinum Nanocatalysts for Toluene Oxidation. ACS Catalysis, 2019, 9, 7431-7442.	5.5	127
17	Enhanced Microwave Absorption Properties by Tuning Cation Deficiency of Perovskite Oxides of Two-Dimensional LaFeO ₃ /C Composite in X-Band. ACS Applied Materials & Interfaces, 2017, 9, 7601-7610.	4.0	123
18	A Universal Strategy toward the Precise Regulation of Initial Coulombic Efficiency of Liâ€Rich Mnâ€Based Cathode Materials. Advanced Materials, 2021, 33, e2103173.	11.1	116

#	Article	IF	CITATIONS
19	3D Ferroconcreteâ€Like Aminated Carbon Nanotubes Network Anchoring Sulfur for Advanced Lithium–Sulfur Battery. Advanced Energy Materials, 2018, 8, 1801066.	10.2	115
20	Template-Free Synthesis of Amorphous Double-Shelled Zinc–Cobalt Citrate Hollow Microspheres and Their Transformation to Crystalline ZnCo ₂ O ₄ Microspheres. ACS Applied Materials & Interfaces, 2013, 5, 5508-5517.	4.0	114
21	Electrostatic Assembly of Sandwich-like Ag-C@ZnO-C@Ag-C Hybrid Hollow Microspheres with Excellent High-Rate Lithium Storage Properties. ACS Nano, 2016, 10, 1283-1291.	7.3	109
22	Enhanced electrochemical performances of layered-spinel heterostructured lithium-rich Li1.2Ni0.13Co0.13Mn0.54O2 cathode materials. Chemical Engineering Journal, 2019, 370, 499-507.	6.6	106
23	Fabrication and understanding of Cu ₃ Si-Si@carbon@graphene nanocomposites as high-performance anodes for lithium-ion batteries. Nanoscale, 2018, 10, 22203-22214.	2.8	103
24	Facile synthesis and microwave absorption properties of yolk-shell ZnO-Ni-C/RGO composite materials. Chemical Engineering Journal, 2018, 333, 92-100.	6.6	102
25	Boosting the potassium-ion storage performance enabled by engineering of hierarchical MoSSe nanosheets modified with carbon on porous carbon sphere. Science Bulletin, 2022, 67, 933-945.	4.3	96
26	Enhanced microwave absorption properties in GHz range of Fe3O4/C composite materials. Journal of Alloys and Compounds, 2015, 649, 537-543.	2.8	95
27	Anchoring Polysulfides and Accelerating Redox Reaction Enabled by Feâ€Based Compounds in Lithium–Sulfur Batteries. Advanced Functional Materials, 2021, 31, 2100970.	7.8	94
28	Multifunctional roles of carbonâ€based hosts for Liâ€metal anodes: A review. , 2021, 3, 303-329.		93
29	First application of core-shell Ag@Ni magnetic nanocatalyst for transfer hydrogenation reactions of aromatic nitro and carbonyl compounds. RSC Advances, 2013, 3, 1050-1054.	1.7	84
30	Dual Electrostatic Assembly of Graphene Encapsulated Nanosheetâ€Assembled ZnOâ€Mn Hollow Microspheres as a Lithium Ion Battery Anode. Advanced Functional Materials, 2018, 28, 1707433.	7.8	83
31	Copper-Nanoparticle-Induced Porous Si/Cu Composite Films as an Anode for Lithium Ion Batteries. ACS Nano, 2017, 11, 6893-6903.	7.3	82
32	Manipulating the Local Electronic Structure in Liâ€Rich Layered Cathode Towards Superior Electrochemical Performance. Advanced Functional Materials, 2021, 31, 2100783.	7.8	79
33	Uniform Na ⁺ Dopingâ€Induced Defects in Li―and Mnâ€Rich Cathodes for Highâ€Performance Lithiumâ€Ion Batteries. Advanced Science, 2019, 6, 1802114.	5.6	78
34	Chemisorption and electrocatalytic effect from CoxSny alloy for high performance lithium sulfur batteries. Energy Storage Materials, 2019, 23, 62-71.	9.5	76
35	3D lithiophilic–lithiophobic–lithiophilic dual-gradient porous skeleton for highly stable lithium metal anode. Journal of Materials Chemistry A, 2020, 8, 313-322.	5.2	76
36	3D uniform nitrogen-doped carbon skeleton for ultra-stable sodium metal anode. Nano Research, 2020, 13, 2136-2142.	5.8	75

#	Article	IF	CITATIONS
37	Structural and magnetic characteristics of monodispersed Fe and oxide-coated Fe cluster assemblies. Journal of Applied Physics, 2002, 92, 3075-3083.	1.1	74
38	Scalable Synthesis of Pore-Rich Si/C@C Core–Shell-Structured Microspheres for Practical Long-Life Lithium-Ion Battery Anodes. ACS Applied Materials & Interfaces, 2022, 14, 10308-10318.	4.0	73
39	Structure, optical and magnetic properties of Ni@Au and Au@Ni nanoparticles synthesized via non-aqueous approaches. Journal of Materials Chemistry, 2012, 22, 2757-2765.	6.7	70
40	Co ₂ P Nanorods as an Efficient Cocatalyst Decorated Porous gâ€C ₃ N ₄ Nanosheets for Photocatalytic Hydrogen Production under Visible Light Irradiation. Particle and Particle Systems Characterization, 2018, 35, 1700251.	1.2	69
41	One-pot synthesis of hexagonal and triangular nickel–copper alloy nanoplates and their magnetic and catalytic properties. Journal of Materials Chemistry, 2012, 22, 8336.	6.7	66
42	Facile synthesis of Fe 3 O 4 /C composites for broadband microwave absorption properties. Applied Surface Science, 2018, 445, 82-88.	3.1	65
43	Stable Nanoâ€Encapsulation of Lithium Through Seedâ€Free Selective Deposition for Highâ€Performance Li Battery Anodes. Advanced Energy Materials, 2020, 10, 1902956.	10.2	65
44	Synthesis of ZnO–ZnCo2O4 hybrid hollow microspheres with excellent lithium storage properties. Electrochimica Acta, 2015, 169, 283-290.	2.6	64
45	Blue luminescence from Ce-doped ZnO thin films prepared by magnetron sputtering. Applied Physics A: Materials Science and Processing, 2012, 108, 239-245.	1.1	63
46	Self-assembly synthesis of 3D graphene-encapsulated hierarchical Fe 3 O 4 nano-flower architecture with high lithium storage capacity and excellent rate capability. Journal of Power Sources, 2017, 365, 98-108.	4.0	61
47	3D Graphene Encapsulated Hollow CoSnO ₃ Nanoboxes as a High Initial Coulombic Efficiency and Lithium Storage Capacity Anode. Small, 2018, 14, 1703513.	5.2	60
48	Engineering oxygen vacancies in hierarchically Li-rich layered oxide porous microspheres for high-rate lithium ion battery cathode. Science China Materials, 2019, 62, 1374-1384.	3.5	58
49	High-Energy and High-Power Pseudocapacitor–Battery Hybrid Sodium-Ion Capacitor with Na+ Intercalation Pseudocapacitance Anode. Nano-Micro Letters, 2021, 13, 55.	14.4	58
50	Hierarchical ZnO–Ag–C Composite Porous Microspheres with Superior Electrochemical Properties as Anode Materials for Lithium Ion Batteries. ACS Applied Materials & Interfaces, 2014, 6, 19895-19904.	4.0	56
51	Synthesis and characterization of the SnS nanowires via chemical vapor deposition. Applied Physics A: Materials Science and Processing, 2012, 106, 87-91.	1.1	53
52	Synthesis, Optical Properties and Photovoltaic Application of the SnS Quasi-one-dimensional Nanostructures. Nano-Micro Letters, 2013, 5, 1-6.	14.4	53
53	Facile preparation and microwave absorption properties of porous Co/CoO microrods. Journal of Alloys and Compounds, 2017, 721, 411-418.	2.8	52
54	Phosphorus-Doped Metal–Organic Framework-Derived CoS ₂ Nanoboxes with Improved Adsorption-Catalysis Effect for Li–S Batteries. ACS Applied Materials & Interfaces, 2021, 13, 15226-15236.	4.0	51

#	Article	IF	CITATIONS
55	An Ultrahighâ€Power Mesocarbon Microbeads Na ⁺ â€Ðiglyme Na ₃ V ₂ (PO ₄) ₃ Sodiumâ€Ion Battery. Advanced Materials, 2022, 34, e2108304.	11.1	50
56	Magnetic properties and magnetoresistance in small iron oxide cluster assemblies. Applied Physics Letters, 2002, 81, 4598-4600.	1.5	49
57	One-pot fabrication of graphene sheets decorated Co2P-Co hollow nanospheres for advanced lithium ion battery anodes. Electrochimica Acta, 2017, 232, 465-473.	2.6	49
58	SnS homojunction nanowire-based solar cells. Journal of Materials Chemistry, 2012, 22, 16437.	6.7	48
59	Electrochemically induced highly ion conductive porous scaffolds to stabilize lithium deposition for lithium metal anodes. Journal of Materials Chemistry A, 2019, 7, 11683-11689.	5.2	47
60	Surface Ni-rich engineering towards highly stable Li1.2Mn0.54Ni0.13Co0.13O2 cathode materials. Energy Storage Materials, 2020, 25, 76-85.	9.5	47
61	Facile fabrication of various zinc-nickel citrate microspheres and their transformation to ZnO-NiO hybrid microspheres with excellent lithium storage properties. Scientific Reports, 2015, 5, 8351.	1.6	46
62	Conductive polyaniline doped with phytic acid as a binder and conductive additive for a commercial silicon anode with enhanced lithium storage properties. Journal of Materials Chemistry A, 2020, 8, 16323-16331.	5.2	46
63	Unprecedented and highly stable lithium storage capacity of (001) faceted nanosheet-constructed hierarchically porous TiO2/rGO hybrid architecture for high-performance Li-ion batteries. National Science Review, 2020, 7, 1046-1058.	4.6	46
64	Facile synthesis of Li-rich layered oxides with spinel-structure decoration as high-rate cathode for lithium-ion batteries. Electrochimica Acta, 2019, 299, 844-852.	2.6	41
65	High Initial Reversible Capacity and Long Life of Ternary SnO2-Co-carbon Nanocomposite Anodes for Lithium-Ion Batteries. Nano-Micro Letters, 2019, 11, 18.	14.4	41
66	Lithium Fluoride Coated Silicon Nanocolumns as Anodes for Lithium Ion Batteries. ACS Applied Materials & Interfaces, 2020, 12, 18465-18472.	4.0	41
67	Mechanisms and applications of layer/spinel phase transition in Li- and Mn-rich cathodes for lithium-ion batteries. Rare Metals, 2022, 41, 1456-1476.	3.6	41
68	Lithium-rich layered oxide nanowires bearing porous structures and spinel domains as cathode materials for lithium-ion batteries. Journal of Power Sources, 2019, 418, 122-129.	4.0	40
69	Dendriteâ€Free Reverse Lithium Deposition Induced by Ion Rectification Layer toward Superior Lithium Metal Batteries. Advanced Functional Materials, 2021, 31, 2104081.	7.8	39
70	ZnO/Ni/C composite hollow microspheres as anode materials for lithium ion batteries. Journal of Alloys and Compounds, 2015, 619, 235-239.	2.8	37
71	Composition- and Structure-Tunable Gold–Cobalt Nanoparticles and Electrocatalytic Synergy for Oxygen Evolution Reaction. ACS Applied Materials & Interfaces, 2016, 8, 20082-20091.	4.0	36
72	Recent developments and challenges of Li-rich Mn-based cathode materials for high-energy lithium-ion batteries. Materials Today Energy, 2020, 18, 100518.	2.5	36

#	Article	IF	CITATIONS
73	Hierarchical Design of Mn ₂ P Nanoparticles Embedded in N,P-Codoped Porous Carbon Nanosheets Enables Highly Durable Lithium Storage. ACS Applied Materials & Interfaces, 2020, 12, 36247-36258.	4.0	36
74	Synthesis of amorphous ZnSnO3 double-shell hollow microcubes as advanced anode materials for lithium ion batteries. Electrochimica Acta, 2015, 182, 327-333.	2.6	35
75	Shape-dependent magnetic and microwave absorption properties of iron oxide nanocrystals. Materials Chemistry and Physics, 2017, 192, 339-348.	2.0	35
76	3D graphene-encapsulated hierarchical urchin-like Fe 3 O 4 porous particles with enhanced lithium storage properties. Chemical Engineering Journal, 2017, 327, 678-685.	6.6	35
77	Sodiophilic Zn/SnO2 porous scaffold to stabilize sodium deposition for sodium metal batteries. Chemical Engineering Journal, 2021, 404, 126469.	6.6	35
78	Homogeneous bottom-growth of lithium metal anode enabled by double-gradient lithiophilic skeleton. Journal of Energy Chemistry, 2021, 57, 392-400.	7.1	35
79	Multi-strategy synergistic Li-rich layered oxides with fluorine-doping and surface coating of oxygen vacancy bearing CeO2 to achieve excellent cycling stability. Chemical Engineering Journal, 2022, 431, 133799.	6.6	35
80	Characteristic tunnel-type conductivity and magnetoresistance in a CoO-coated monodispersive Co cluster assembly. Applied Physics Letters, 1999, 74, 76-78.	1.5	34
81	High-Performance Na–O ₂ Batteries Enabled by Oriented NaO ₂ Nanowires as Discharge Products. Nano Letters, 2018, 18, 3934-3942.	4.5	33
82	Magnetic softness and high-frequency characteristics of Fe65Co35–O alloy films. Journal of Applied Physics, 2009, 106, 013912.	1.1	32
83	Constructing Robust Cross-Linked Binder Networks for Silicon Anodes with Improved Lithium Storage Performance. ACS Applied Materials & Interfaces, 2021, 13, 53818-53828.	4.0	32
84	Challenge and Strategies in Room Temperature Sodium–Sulfur Batteries: A Comparison with Lithium–Sulfur Batteries. Small, 2022, 18, e2107368.	5.2	32
85	Disproportionation route to monodispersed copper nanoparticles for the catalytic synthesis of propargylamines. RSC Advances, 2013, 3, 19812.	1.7	31
86	Synthesis of ZnO-Cu-C yolk-shell hybrid microspheres with enhanced electrochemical properties for lithium ion battery anodes. Electrochimica Acta, 2017, 226, 79-88.	2.6	31
87	Bottom-top channeling Li nucleation and growth by a gradient lithiophilic 3D conductive host for highly stable Li-metal anodes. Journal of Materials Chemistry A, 2020, 8, 1678-1686.	5.2	31
88	Ion Reservoir Enabled by Hierarchical Bimetallic Sulfides Nanocages Toward Highly Effective Sodium Storage. Small, 2020, 16, e1907261.	5.2	31
89	Construction of Sb ₂ S ₃ @SnS@C Tubular Heterostructures as High-Performance Anode Materials for Sodium-Ion Batteries. ACS Sustainable Chemistry and Engineering, 2021, 9, 11280-11289.	3.2	31
90	Core–shell zeolite imidazole framework-derived ZnSe@CoSe2/C heterostructure enabling robust polysulfide adsorption and rapid Li+ diffusion in high-rate and high-loading lithium–sulfur batteries. Chemical Engineering Journal, 2022, 430, 133099.	6.6	31

#	Article	IF	CITATIONS
91	Rational integration of spatial confinement and polysulfide conversion catalysts for high sulfur loading lithium–sulfur batteries. Nanoscale Horizons, 2020, 5, 720-729.	4.1	30
92	Designing Polymerâ€inâ€Salt Electrolyte and Fully Infiltrated 3D Electrode for Integrated Solidâ€State Lithium Batteries. Angewandte Chemie, 2021, 133, 13041-13050.	1.6	30
93	Composite deposition of Co and Si clusters by rf/dc plasma-gas-codensation. Applied Physics Letters, 2003, 82, 2688-2690.	1.5	28
94	Boosting the Electrochemical Performance of Li- and Mn-Rich Cathodes by a Three-in-One Strategy. Nano-Micro Letters, 2021, 13, 205.	14.4	28
95	Cu ₄ SnS ₄ -Rich Nanomaterials for Thin-Film Lithium Batteries with Enhanced Conversion Reaction. ACS Nano, 2019, 13, 10671-10681.	7.3	26
96	Composite NiCo ₂ O ₄ @CeO ₂ Microsphere as Cathode Catalyst for Highâ€Performance Lithium–Oxygen Battery. Advanced Science, 2022, 9, e2200523.	5.6	26
97	Enhanced Cyclability of Lithium Metal Anodes Enabled by Anti-aggregation of Lithiophilic Seeds. Nano Letters, 2022, 22, 5874-5882.	4.5	26
98	Formation and magnetic properties of Fe–Pt alloy clusters by plasma-gas condensation. Applied Physics Letters, 2003, 83, 350-352.	1.5	25
99	Electron transport properties of magnetic granular films. Science China: Physics, Mechanics and Astronomy, 2013, 56, 15-28.	2.0	25
100	High performance of Ge@C nanocables as the anode for lithium ion batteries. RSC Advances, 2014, 4, 21450-21455.	1.7	25
101	From a Au-rich core/PtNi-rich shell to a Ni-rich core/PtAu-rich shell: an effective thermochemical pathway to nanoengineering catalysts for fuel cells. Journal of Materials Chemistry A, 2018, 6, 5143-5155.	5.2	25
102	Promising Electrode and Electrolyte Materials for Highâ€Energyâ€Density Thinâ€Film Lithium Batteries. Energy and Environmental Materials, 2022, 5, 133-156.	7.3	25
103	Morphology Control and Na ⁺ Doping toward High-Performance Li-Rich Layered Cathode Materials for Lithium-Ion Batteries. ACS Sustainable Chemistry and Engineering, 2021, 9, 197-206.	3.2	25
104	Magnetic and electrical properties of Feâ^•Si core-shell cluster assemblies prepared with double-glow-discharge sources. Applied Physics Letters, 2005, 87, 252501.	1.5	23
105	Multiscale Deficiency Integration by Na-Rich Engineering for High-Stability Li-Rich Layered Oxide Cathodes. ACS Applied Materials & Interfaces, 2021, 13, 8239-8248.	4.0	23
106	Solution synthesis of triangular and hexagonal nickel nanosheets with the aid of tungsten hexacarbonyl. CrystEngComm, 2016, 18, 1295-1301.	1.3	22
107	Synthesis of Cu2O mesocrystal and its application in photocatalysis. Applied Physics A: Materials Science and Processing, 2015, 118, 763-767.	1.1	21
108	Utilizing the different distribution habit of La and Zr in Li-rich Mn-based cathode to achieve fast lithium-ion diffusion kinetics. Journal of Power Sources, 2021, 499, 229915.	4.0	21

#	Article	IF	CITATIONS
109	3D graphene encapsulated ZnO-NiO-CuO double-shelled hollow microspheres with enhanced lithium storage properties. Journal of Alloys and Compounds, 2018, 765, 1158-1166.	2.8	19
110	Li–Zn Overlayer to Facilitate Uniform Lithium Deposition for Lithium Metal Batteries. ACS Applied Materials & Interfaces, 2021, 13, 9985-9993.	4.0	19
111	MoSe2-Ni3Se4 Hybrid Nanoelectrocatalysts and Their Enhanced Electrocatalytic Activity for Hydrogen Evolution Reaction. Nanoscale Research Letters, 2020, 15, 132.	3.1	19
112	Co cluster coalescence behavior observed by electrical conduction and transmission electron microscopy. Applied Physics Letters, 2001, 78, 1535-1537.	1.5	18
113	Multistage Li _{1.2} Ni _{0.2} Mn _{0.6} O ₂ Microâ€architecture towards Highâ€Performance Cathode Materials for Lithiumâ€ion Batteries. ChemElectroChem, 2017, 4, 3250-3256.	1.7	17
114	Ion―and Electronâ€Conductive Buffering Layerâ€Modified Si Film for Use as a Highâ€Rate Longâ€Term Lithiumâ€Ion Battery Anode. ChemSusChem, 2019, 12, 252-260.	3.6	17
115	Enhancing cycling stability in Li-rich Mn-based cathode materials by solid-liquid-gas integrated interface engineering. Nano Energy, 2022, 97, 107201.	8.2	17
116	Colloidal synthesis of Cu–ZnO and Cu@CuNi–ZnO hybrid nanocrystals with controlled morphologies and multifunctional properties. Nanoscale, 2016, 8, 11602-11610.	2.8	15
117	Preparation of porous Li1.2Mn0.54Ni0.13Co0.13O2 micro-cubes for high-capacity lithium-ion batteries. Journal of Alloys and Compounds, 2020, 834, 155152.	2.8	15
118	A facile approach to fabrication of well-dispersed NiO–ZnO composite hollow microspheres. RSC Advances, 2013, 3, 24430-24439.	1.7	14
119	Regulating Li+ migration and Li2S deposition by metal-organic framework-derived Co4S3-embedded carbon nanoarrays for durable lithium-sulfur batteries. Science China Materials, 2022, 65, 947-957.	3.5	14
120	Metal-organic frameworks-derived hollow dodecahedral carbon combined with FeNx moieties and ruthenium nanoparticles as cathode electrocatalyst for lithium oxygen batteries. Journal of Colloid and Interface Science, 2021, 596, 1-11.	5.0	13
121	Surface Spinel-Coated and Polyanion-Doped Co-Free Li-Rich Layered Oxide Cathode for High-Performance Lithium-Ion Batteries. Industrial & Engineering Chemistry Research, 2022, 61, 7464-7473.	1.8	13
122	Morphology and Magnetic Properties of Fe and Al Nanocomposites Prepared with Single and Double-Glow-Discharge Sources. Materials Transactions, 2008, 49, 1830-1835.	0.4	12
123	Function and Application of Defect Chemistry in Highâ€Capacity Electrode Materials for Liâ€Based Batteries. Chemistry - an Asian Journal, 2020, 15, 3620-3636.	1.7	12
124	Electron transport properties in Nb and NbN cluster-assembled films produced by a plasma–gas–condensation cluster source. Journal of Applied Physics, 2003, 94, 7594.	1.1	11
125	A Layered Lithiumâ€Rich Li(Li _{0.2} Ni _{0.15} Mn _{0.55} Co _{0.1})O ₂ Cathode Material: Surface Phase Modification and Enhanced Electrochemical Properties for Lithium″on Batteries. ChemElectroChem. 2019. 6. 1542-1551.	1.7	10
126	A novel morphology-controlled synthesis of Na+-doped Li- and Mn-rich cathodes by the self-assembly of amphiphilic spherical micelles. Sustainable Materials and Technologies, 2020, 25, e00171.	1.7	10

#	Article	IF	CITATIONS
127	Manipulating External Electric Field and Tensile Strain toward High Energy Density Stability in Fast-Charging Li-Rich Cathode Materials. Journal of Physical Chemistry Letters, 2020, 11, 2322-2329.	2.1	10
128	Intrinsic performance regulation in hierarchically porous Co3O4 microrods towards high-rate lithium ion battery anode. Materials Today Energy, 2020, 16, 100383.	2.5	10
129	Facile fabrication of ZnO–CuO porous hybrid microspheres as lithium ion battery anodes with enhanced cyclability. Rare Metals, 2017, 36, 403-410.	3.6	9
130	Electrochemically induced high ion and electron conductive interlayer in porous multilayer Si film anode with enhanced lithium storage properties. Journal of Power Sources, 2021, 481, 228833.	4.0	9
131	Composite state control and magnetic properties of Co and Si cluster assemblies prepared with double-glow-discharge sources. Journal of Applied Physics, 2006, 100, 034308.	1.1	8
132	Integrated On-Chip Solenoid Inductors With Nanogranular Magnetic Cores. IEEE Transactions on Magnetics, 2016, 52, 1-4.	1.2	8
133	Size-dependent electrical transport properties in Co nanocluster-assembled granular films. Scientific Reports, 2017, 7, 11666.	1.6	8
134	Gas-phase preparation and size control of Fe nanoparticles. Applied Physics A: Materials Science and Processing, 2011, 103, 1015-1020.	1.1	7
135	Structure of Iron/Nickel Composite Cluster Assemblies Prepared by Double Clow-Discharge-Sources. Materials Transactions, 2006, 47, 1949-1952.	0.4	6
136	Electrical transport properties in Co nanocluster-assembled granular film. Journal of Applied Physics, 2017, 121, .	1.1	6
137	A Guideline for Tailoring Lattice Oxygen Activity in Lithium-Rich Layered Cathodes by Strain. Journal of Physical Chemistry Letters, 2019, 10, 2202-2207.	2.1	6
138	Nickel Colloidal Superparticles: Microemulsion-Based Self-Assembly Preparation and Their Transition from Room-Temperature Superparamagnetism to Ferromagnetism. Journal of Physical Chemistry C, 2021, 125, 5880-5889.	1.5	6
139	Effects of O ₂ Gas on the Size and Structure of Cr Clusters Formed by Plasma-Gas-Condensation. Materials Transactions, 2001, 42, 1480-1484.	0.4	5
140	Ferromagnetic, transparent and conducting ITO-Fe-cluster composite films. IEEE Transactions on Magnetics, 2005, 41, 3406-3408.	1.2	5
141	Magnetic and electrical characteristics in dense Fe–Ni alloy cluster-assembled films prepared by energetic cluster deposition. Journal of Materials Research, 2008, 23, 189-197.	1.2	5
142	Fe/Ni Cluster Hybrid Material Produced by Double Glow Discharge Sources. Materials Transactions, 2009, 50, 516-522.	0.4	5
143	High-frequency magnetic characteristics of Fe-Co-based nanocrystalline alloy films. Science China Technological Sciences, 2010, 53, 1501-1506.	2.0	5
144	Interfacial-scattering–induced enhancement of the anomalous Hall effect in uniform Fe nanocluster-assembled films. Europhysics Letters, 2015, 109, 17012.	0.7	5

#	Article	IF	CITATIONS
145	Hot-injection synthesis of Ni-ZnO hybrid nanocrystals with tunable magnetic properties and enhanced photocatalytic activity. Journal of Nanoparticle Research, 2017, 19, 1.	0.8	5
146	Tungsten hexacarbonyl-induced growth of nickel nanorods and nanocubes. Materials Letters, 2018, 229, 340-343.	1.3	5
147	Synthesis and characterization of ferromagnetic transparent conductive films. Materials Chemistry and Physics, 2009, 117, 224-227.	2.0	4
148	High Frequency Characteristics of Fe65Co35 Alloy Cluster-Assembled Films Prepared by Energetic Cluster Deposition. Journal of Nanoscience and Nanotechnology, 2011, 11, 11119-11123.	0.9	4
149	Structure and magnetic properties of the Co x Pt100â^'x nanowire arrays. Applied Physics A: Materials Science and Processing, 2013, 112, 869-875.	1.1	4
150	Photocatalysis: Co2 P Nanorods as an Efficient Cocatalyst Decorated Porous g-C3 N4 Nanosheets for Photocatalytic Hydrogen Production under Visible Light Irradiation (Part. Part. Syst. Charact. 1/2018). Particle and Particle Systems Characterization, 2018, 35, 1870003.	1.2	4
151	Sputtering Coating of Lithium Fluoride Film on Lithium Cobalt Oxide Electrodes for Reducing the Polarization of Lithium-Ion Batteries. Nanomaterials, 2021, 11, 3393.	1.9	4
152	CoP@C with chemisorption-catalysis effect toward lithium polysulfides as multifunctional interlayer for high-performance lithium-sulfur batteries. Electrochimica Acta, 2022, 419, 140391.	2.6	4
153	Magnetic properties of [Fe65Co35–O/SiO2] n multilayer thin films for high-frequency application. Applied Physics A: Materials Science and Processing, 2013, 111, 569-574.	1.1	3
154	Evolution of interfacial structure of the joints between a tungsten-copper composite and austenitic stainless steel. Materials Research Express, 2021, 8, 016514.	0.8	3
155	Challenges and Recent Advances in High Capacity Liâ€Rich Cathode Materials for High Energy Density Lithiumâ€Ion Batteries (Adv. Mater. 50/2021). Advanced Materials, 2021, 33, .	11.1	3
156	Preparation of LiNi0.5Mn1.5O4 cathode materials by using different-sized Mn3O4 nanocrystals as precursors. Journal of Solid State Electrochemistry, 2022, 26, 1359-1368.	1.2	3
157	Formation and characterization of high-density FeÂcluster-assembled films with soft magnetic behaviors. European Physical Journal D, 2005, 34, 173-176.	0.6	2
158	Face-Centered Cubic Ti Cluster Assemblies Prepared by Plasma-Gas-Condensation. Materials Transactions, 2008, 49, 522-526.	0.4	2
159	High Frequency Magnetic Property of Dense Fe ₂₂ Ni ₇₈ Cluster Assembled Films. Materials Transactions, 2009, 50, 664-670.	0.4	2
160	Gas-phase synthesis and magnetism of HfO2 nanoclusters. European Physical Journal D, 2013, 67, 1.	0.6	2
161	Effect of in situ low-temperature annealing on anomalous Hall effect in Co nanocluster-assembled granular film. Journal of Alloys and Compounds, 2018, 748, 922-928.	2.8	2
162	Lithium Batteries: Stable Nanoâ€Encapsulation of Lithium Through Seedâ€Free Selective Deposition for Highâ€Performance Li Battery Anodes (Adv. Energy Mater. 7/2020). Advanced Energy Materials, 2020, 10, 2070031.	10.2	2

#	Article	IF	CITATIONS
163	Atomic mechanisms of hexagonal close-packed Ni nanocrystallization revealed by in situ liquid cell transmission electron microscopy. Nano Research, 2022, 15, 6772-6778.	5.8	2
164	Crystal Structure of Fe-N Clusters Prepared by Plasma-Gas-Condensation. Materials Transactions, 2003, 44, 677-680.	0.4	1
165	Highly Stable Metalâ€Free Longâ€Persistent Luminescent Copolymer for Low Flicker AC‣EDs. Angewandte Chemie, 2022, 134, .	1.6	1
166	Temperature Dependence of Cluster-cluster Coalescence in Monodispersed Co Cluster Assemblies. Materials Research Society Symposia Proceedings, 2001, 676, 3161.	0.1	0
167	Preparation and magnetic properties of size-monodispersed Fe-Co alloy nanoclusters. , 2008, , .		0
168	Core/Shell Morphology in Ti Clusters Prepared by Plasma Gas Condensation and Post Annealing. Materials Transactions, 2009, 50, 523-527.	0.4	0
169	High frequency characteristics of Fe <inf>65</inf> Co <inf>35</inf> alloy cluster-assembled films prepared by energetic cluster deposition. , 2010, , .		0
170	Preparation and characterization of the ZnO:Al/Fe65Co35/ZnO:Al multifunctional films. Applied Physics A: Materials Science and Processing, 2012, 106, 717-723.	1.1	0
171	Anomalous Hall effect in CoxSi1â^'x granular films deposited by magnetron co-sputtering. Journal of Materials Science: Materials in Electronics, 2018, 29, 9814-9820.	1.1	0